

# Reverse engineering applied to a lumbar vertebra

André Lupi, Zdenka Sant

## Abstract

Bone studies can be made *in vivo* or *in vitro*. However, disadvantages of both traditional techniques call for a compromise between the two. Reverse engineering allows *in vitro* bone samples to be simulated and analysed in a virtual *in vivo* environment thus offering a middle ground solution and a sound foundation on which biomechanical studies of bone could develop.

The information derived from the solution of a virtual finite element model, in conjunction with a concrete understanding of the pathophysiology of bone and abnormal skeletal development grants the opportunity for engineering solutions to be applied to skeletal structures in order to predict/prevent fractures and facilitate procedures in orthopedic surgery.<sup>1</sup>

## Keywords

Biomechanics, finite element analysis, lumbar vertebrae, orthopaedics

**André Lupi\*** BMech Eng(Hons)  
Department of Manufacturing Engineering, University of Malta  
University of Malta  
Email: andrelupi84@gmail.com

**Zdenka Sant** MSc(VUT Brno)  
Department of Mechanical Engineering, University of Malta  
Email: zdsant@eng.um.edu.mt

\* corresponding author

## Introduction

### Statistics

Epidemiological studies indicate an unprecedented rise in vertebral column fracture with quoted rates of vertebral body compression fracture ranging from 25% - 50%.<sup>2</sup> Furthermore, it is not always appreciated that vertebral fractures are associated with 28% mortality over 5 years.<sup>3</sup>

Bone density measurements appear to have only a moderate correlation with vertebral body fractures. In the NORA study, 50% of postmenopausal women who developed a vertebral body fracture were osteopenic rather than osteoporotic.<sup>4</sup> Furthermore, fracture intervention studies such as the VERT, FIT and MORE studies, indicate that the fracture reduction attributable to the increases in bone density ranges from only 4% - 28%.<sup>5-7</sup>

*In vitro* and *in vivo* tests conducted on bone samples help experts to understand such statistics by analyzing the variables related to bone strength and function.

### Experiments

*In vitro* experiments are responsible for most of the information on bone and cartilage cell interactions at hand. The material properties and structure of tissue are best investigated through dissection and only after this data is recorded could mechanical computations be conducted on the sample. *In vitro* testing requires the sample tissue to be prepared beforehand. This 'cleaning' process is known to affect the empirical results. Consequently, results from studies of similar bones through alternative procedures would vary. Observed responses of *in vitro* experiments may not reflect the actual *in vivo* analysis since the environmental factors differ.

The measurement and testing of biological tissue could be conducted in an alternative way. *In vivo* experiments have only been recently developed and are conducted with the aid of scanned images. In contrast to *in vitro* tests, they are more suited to deduce the mechanisms of action of biological components. However, a limited control over the variables could confound the experiment leading to ambiguous or unreliable results.<sup>8</sup>

Computed Tomography (CT), Magnetic Resonance Imaging (MRI) and Dual Energy X-ray Absorptiometry (DEXA) scans are used to conduct *in vivo* studies.<sup>9</sup> The choice of scan depends on various factors such as the quality or resolution of the image required and the type of tissue under test.

By acknowledging the difficulty to compile the required data for the study and correctly interpreting the results from *in vivo* testing and by being aware of the obstacles to conduct an *in vitro* analysis, one can appreciate that a compromise between the two would be ideal. Such a compromise can be attained through Reverse Engineering (RE).

### Definition

RE is the process of discovering the technological properties of any object or a system by analyzing its structure, function and operation.

It presents us with an alternative approach to the two traditional measurement and testing procedures, comprising a computer simulation of the tissue, using the *in vitro* sample to define the bone geometry and simulating the virtual image in an *in vivo* environment. The *in vitro* geometry could be captured through CT, MRI or three-dimensional (3D) laser scanning techniques.

By reverse-engineering a human lumbar vertebra, one can appreciate its clever architecture and the effect of the tissue's anisotropic material properties on load-bearing capabilities (anisotropy is the property of being directionally dependant). An investigation of the strain (deformation of the bone) and stress (force causing deformation) contours induced in the specimen under loading helps identifies areas more susceptible to fracture.

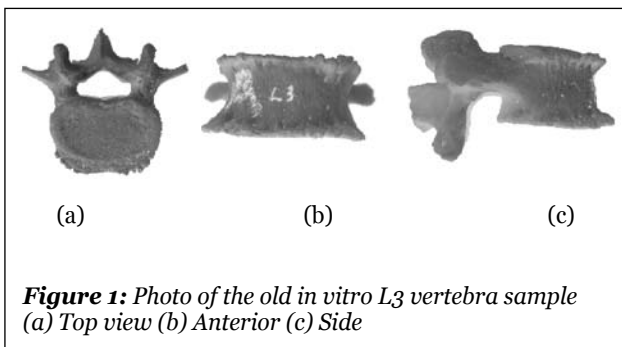


**Figure 1:** Photo of the old *in vitro* L3 vertebra sample (a) Top view (b) Anterior (c) Side

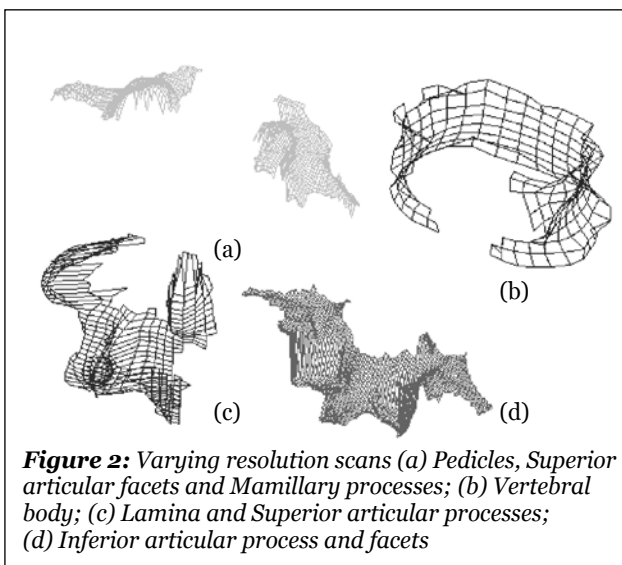


**Figure 2:** Varying resolution scans (a) Pedicles, Superior articular facets and Mamillary processes; (b) Vertebral body; (c) Lamina and Superior articular processes; (d) Inferior articular process and facets

### Method

With an increase in the popularity of Computer-Aided Design (CAD) it is common to reverse-engineer objects or systems through 3D virtual models.<sup>10, 11</sup> The virtual geometry can be obtained using several scanning techniques; namely CT, MRI or 3D laser methods.

The third lumbar vertebra (L3) sample available (Figure 1) was scanned using the latter technique employing the Spot Beam Triangulation scanning method since no other alternative was available.

Despite the scanner's inaccuracy and the disadvantage of scanning a deteriorated specimen, the simple 3D laser scanner was readily available and although not as sophisticated and efficient as MRI or CT equipment, the *in vitro* geometric data recorded proved to be satisfactory. In addition to this, unlike DICOM data extracted from CT or MRI scanning methods, the laser scanner writes the geometric data to an IGES file; the only exchange format compatible with the licensed software available.<sup>12</sup> Such a file format would facilitate data exchange between software applications considerably.

Complex geometry, such as that of the vertebrae, imposed problems with this laser alternative. Since the laser light does not slice or penetrate the tissue, not all points at the surface were targeted. Such blind spots, such as the walls of the vertebral foramen, provided a bulk of missing data, which was difficult to remodel manually due to its original complex profile.

The data was captured from four perspectives (Figure 2) using three resolutions, depending on the complexity of the bone surface (Table 1). The top and bottom faces of the vertebra were

**Table 1:** Varying resolution scan settings

<b>Rotary scan</b>	<b>Circum pitch &amp; height-dir pitch</b>
Vertebral body Lamina,	10 degrees & 2.5400 mm
Superior articular processes	5 degrees & 11.9380 mm
<b>Planar scan</b>	<b>Width-dir pitch &amp; height-dir pitch</b>
Pedicles, Superior articular facets and Mamillary processes	0.6096 & 0.6096 mm
Inferior articular process and facets	0.6096 & 0.6096 mm

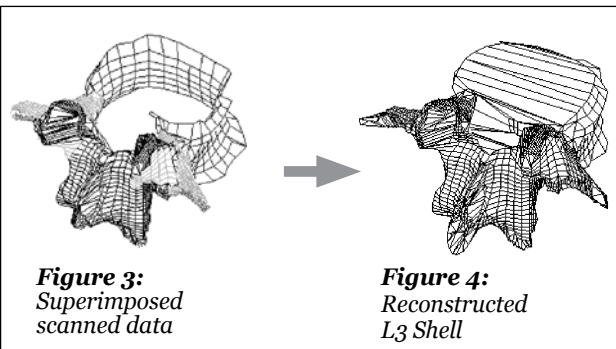


**Figure 3:** Superimposed scanned data

**Figure 4:** Reconstructed L3 Shell

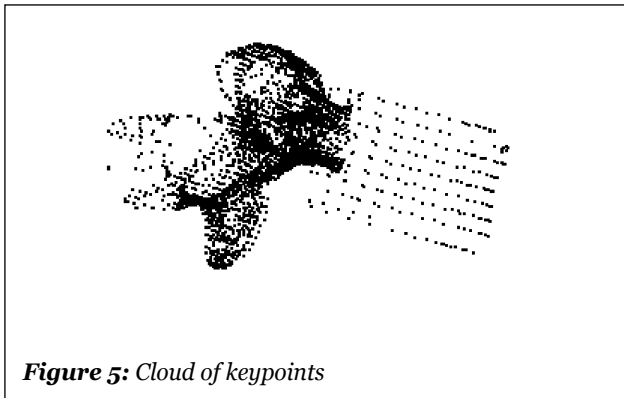


**Figure 5:** Cloud of keypoints

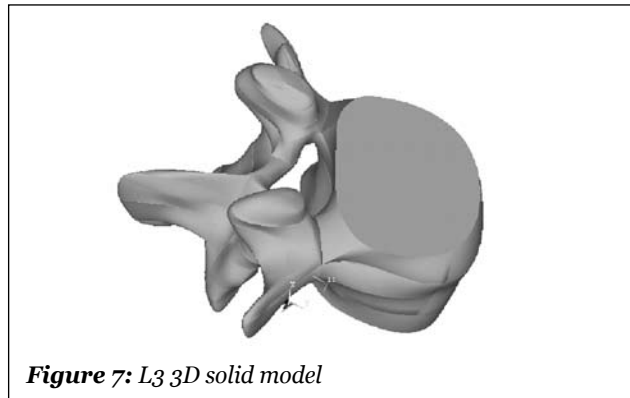


**Figure 7:** L3 3D solid model

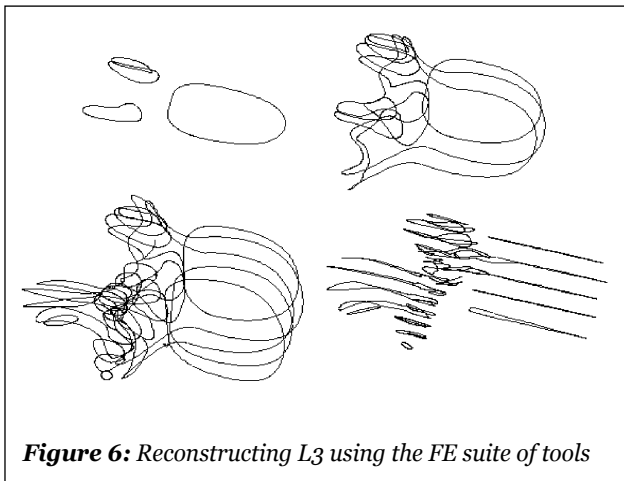


**Figure 6:** Reconstructing L3 using the FE suite of tools

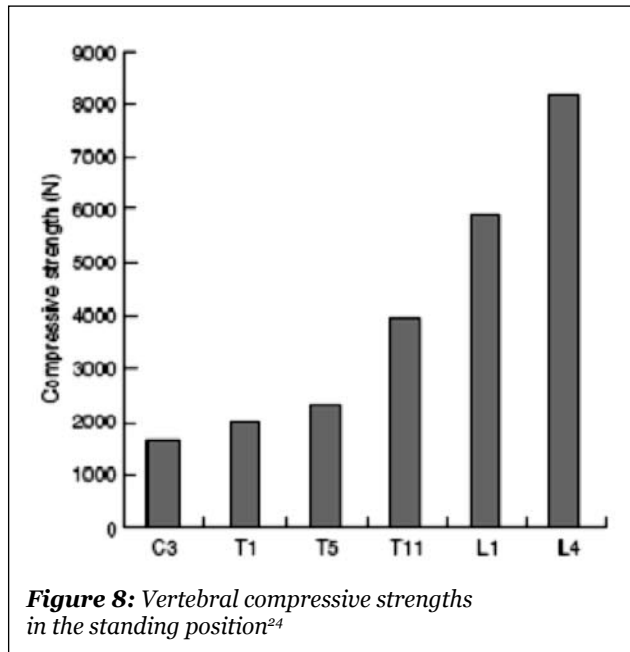


**Figure 8:** Vertebral compressive strengths in the standing position<sup>24</sup>

omitted since these planar areas could be easily reformed with the appropriate CAD editing tools once the four scanned images were superimposed via the CAD application (Figure 3).

The scanned result required the transverse processes, the missing walls of the vertebral foramen, the top and bottom faces of the vertebral body and the spinous process to be remodeled (Figure 4).

The reconstructed CAD shell was transferred to the Finite Element (FE) application via an IGES file and only the cloud of keypoints (Figure 5) was chosen to be kept after import.

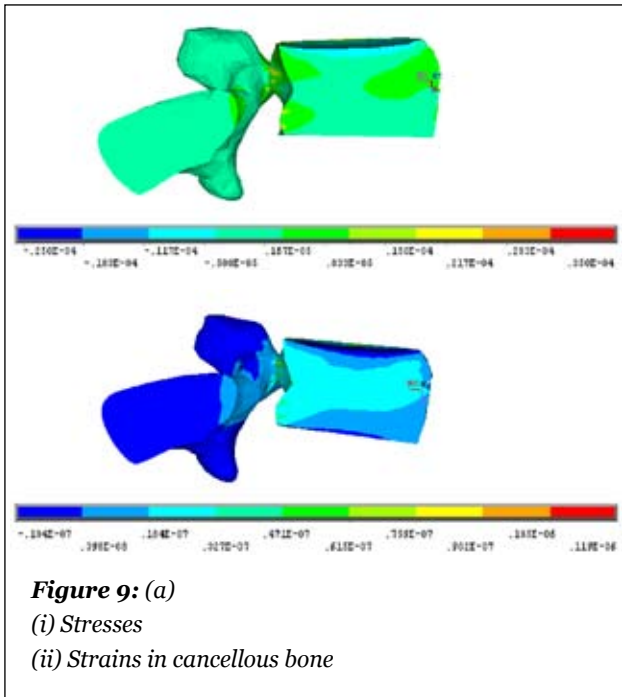
Such points were used to reconstruct the vertebra once more, this time in the FE application (Figure 6), in order to create a 3D solid model of the L3 bone and through the suite

of modeling tools available a smooth, realistic surface was acquired (Figure 7).

Compared to other virtual vertebra models, Figure 7 presents a very realistic image.<sup>13-15</sup> The bone is not symmetrical and changes in the surface gradient are very small, thus presenting a smooth finish with no sharp edges.<sup>16</sup> This detail can only be acquired through RE and is a key factor to obtaining accurate results in order to analyse the structure correctly.

**Table 2:** Material Properties

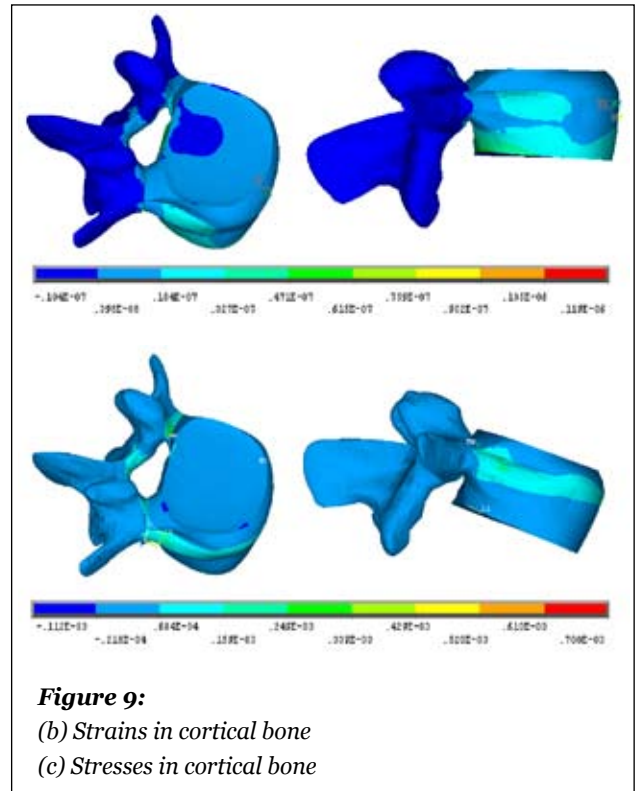
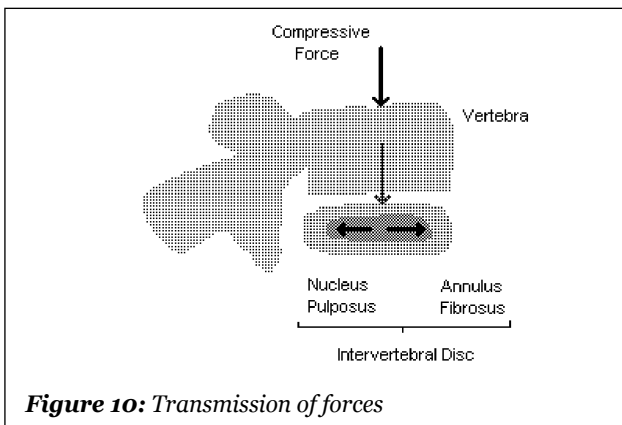
<b>Material Property</b>	<b>Isotropic Cancellous Core<sup>23</sup></b>	<b>Anisotropic Cortical Shell<sup>21, 22</sup></b>
Young's Modulus, E (MPa)	14000	X - 467.88 Y - 196.56 Z - 134.26
Shear Modulus, G (MPa)	9100	XY - 61.18 YZ - 71.68 XZ - 85.54
Poisson's Ratio $\nu$	0.3	XY - 0.381 YZ - 0.226 XZ - 0.399



The next step of this RE procedure was to analyse the bone's behavior in an *in vivo* environment. The model was given its respective material properties (Table 2); it was meshed with triangular elements and was assumed to follow Hooke's law (strain is directly proportional to stress), since the strains developed in the bone are expected to fall in the physiological range.<sup>17</sup> Since the compressive strengths of the vertebrae (figure 8), in the standing position, increase as one moves caudad from the third cervical bone to the fourth lumbar vertebra, a force of 2000N was applied to the superior face of the virtual vertebral body (the limits of these loads are defined by the axial strength of the individual vertebrae).<sup>18</sup> This value is typically used in lumbar vertebrae computations and was therefore deemed fit for the objectives of this study.<sup>19, 20</sup>

The finite element method (FEM) was employed to deduce the structural properties of the two-phase osseous tissue. The deduced results are illustrated in Figure 9.<sup>25</sup>

The cortical shell was not modeled as anisotropic since the data was not available for human bone (researches on human samples are still being carried out) and the age and gender



of the specimen were not available as the material properties were deduced from a range of values. Elastic constants data in literature is always found as a range of results.<sup>26-29</sup> Most elastic constants are usually derived from bovine samples but the ones used for this analysis are human.

## Discussion & results

In contrast to the cortical shell, the cancellous core has a lower elastic modulus giving it better elastic properties. Because of its lattice structure, cancellous bone can tolerate much higher stresses than the dense cortical bone. It is more favorable for load-bearing since the transmitted forces are subdivided into horizontal and vertical components. Thus, it is desirable to have lower stresses on the outer surface by having most of the load being borne by the inner core tissue. Computed results have shown this sought-after effect.

The anisotropic properties of the material also contribute to its load-bearing capabilities and in order to appreciate such property of healthy bone, another computation was made on the same model, with isotropic material properties (results not shown). The new material properties were as follows; Cortical bone EX = 14000MPa, Cancellous bone EX = 160Mpa.

By comparing both models it was noticed that stresses and strain varied significantly, with the same loading conditions. The isotropic model was structurally weaker than the anisotropic one; undesirable high stresses were seen on the cortical shell. This configuration redistributed the forces such that more load was borne by the brittle inelastic tissue. Such a comparison can give an idea of how bone architecture can weaken when bone diseases distort the architectural configuration tending

it to remodel in an isotropic fashion. Paget's disease and osteoporosis are ideal examples of such disordered remodeling sequences, which compromise the load-bearing capabilities of the tissue.

A distorted structural configuration of the vertebral column could also compromise the vertebrae load-bearing capabilities. If a structurally disordered vertebral column were to be scanned, such as in scoliosis or vertebral bone fractures, the RE analysis could unveil points of weakness in the structure and help identify strategic solutions to redistribute the loading on the vertebrae, preventing further deformation, as in the use of Harrington rods and bone grafts.<sup>1</sup>

Professionals could move the surgical apparatus around the 3D model in a virtual environment and by observing changes in the stress and strain distribution the optimum position for the contraption could be deduced. Besides guiding medical professionals, this RE technique can be used to better such surgical apparatus by modifying their designs and testing them virtually before they are manufactured.

In-depth FE analysis of the vertebrae would reveal that not all compressive loads subjected to the L3 bone are borne by that vertebra.<sup>15-19</sup> Ligaments surrounding the vertebrae are designed to distribute the lumbar loading. They transfer part of the load to the thoracic spine and their prestressed properties allow them to maintain a considerable amount of loading in a tensile form within its fibres. Furthermore, the facet joints bear 10% to 40% of the total load within their synovial fluids due to the lumbar vertebra's facet plane angle of 90°. <sup>30</sup> The intervertebral discs in the vertebral column also detract excessive compressive loads away from the vertebral bodies. They comprise a central fluid mass (the nucleus pulposus) encapsulated in a laminated, elastic fibrocartilaginous shell (the annulus fibrosus) and are prestressed. Their structure converts compressive forces transmitted from the vertebrae, into radial forces resisted by the annulus fibrosus making them more oblique through stretching, as energy is stored in the elastic distortion (Figure 10).

RE is also applied in the design of prosthetic applications.<sup>14,31</sup> Healthy bone systems are scanned, analysed and compared to systems comprising artificial limbs or purposely-fused bone in order to improve these non-natural designs, further imitating their natural biological form.

In conclusion Reverse Engineering should provide another method of analyzing variables related to bone strength and function. This method may assist current modes of bone assessments possibly quantifying risk for fracture or bone malfunction.

## Acknowledgements

The author would like to thank Dr Yves Muscat Baron for his input and Ing. Zdenka Sant for her technical assistance. Their support is greatly appreciated.

## References

1. Aubin CÉ, Petit Y, Stokes IAF, Poulin F, Gardner-Morse M and Labelle H. Biomechanical modelling of posterior instrumentation of the scoliotic spine. *Computer Methods in Biomechanics and Biomedical Engineering*. 2003;6:27-32.
2. Johansen A, Evans R, Stone et al. Fracture incidence in England and Wales: a study based on the population of Cardiff. *Injury* 1997;28:655-660.
3. Kanis JA, Oden A, Johnell O, De Laet C, Jonsson B. Excess mortality after hospitalisation for vertebral fracture. *Osteoporos Int* 2004;15:108-12.
4. Siris ES, Chen YT, Abbott TA et al. Bone Mineral Density Thresholds for Pharmacological Intervention to Prevent Fractures. *Arch Intern Med* 2004;164:1047-8.
5. Ettinger B, Black D, Mitlak B et al. The Multiple Outcomes of Raloxifene Evaluation (MORE) Investigations. Reduction of fracture risk for a 3 year randomized clinical study. *JAMA* 1999;282:637-45.
6. Cummings S, Black D, Thompson D et al. The Fracture Intervention Research Group. Effect of alendronate on risk of fracture in women with low bone density but without fractures. Results from the fracture intervention trial. *JAMA* 1998;280:2077-82.
7. Harris S, Watts N, Genant H et al. Vertebral Efficacy with Residronate Therapy (VERT Study Group). Effects of residronate treatment on vertebral and nonvertebral fracture in women with postmenopausal osteoporosis: a randomised controlled trial. *JAMA* 1999;287:1344-52.
8. Mulconrey DS, Knight RQ, Bramble JD, Paknikar S, Harty PA. Interobserver reliability in the interpretation of diagnostic lumbar MRI and nuclear imaging. *The Spine Journal*. 2006;6:177-84.
9. Benno MN and Herzog W, *Biomechanics of the Musculo-skeletal System*. 2nd Ed, Chichester, Wiley, 1999, p. 190.
10. Digital Geometry Processing. Class notes for Siggraph 2001, Caltech Multi-Res Modelling Group, Caltech. Available from <http://www.multires.caltech.edu>
11. Skalski K, Filipowski R, Swieszkowski W, Kedzior K, Dabrowski A, Zawora J. Identification and geometrical modelling of complex shape surfaces using coordinate measuring machine and CAD/CAM systems. *Journal of Materials Processing Technology*.1998;76:49-55.
12. CAD/CAM - Better models, better translations. *Machine Design*. 2000;72:D7. Available from: <http://www.wilsonweb.com>
13. Eberlein R, Holzapfel GA and Frohlich M. Multi-segment FEA of the human lumbar spine including the heterogeneity of the annulus fibrosus. *Journal of Computational Mechanics*. 2004;34:147-63.
14. Rohlmann A, Zander T, Bergmann G. Effects of fusion-bone stiffness on the mechanical behaviour of the lumbar spine after vertebral body replacement. *Clinical Biomechanics*. 2005;21:221-27.
15. Ezquerro F, Simon A, Prado M and Pe´rez A. Combination of finite element modelling and optimization for the study of lumbar spine biomechanics considering the 3D thorax–pelvis orientation. *Medical Engineering & Physics*. 2003;26:11-22.
16. Farin G and Hansford D. Discrete coons patches. *Computer Aided Geometric Design*. 1999;16:691-700.
17. Langton CM and Njeh CF. *The Physical Measurement of Bone*. London, Institute of Physics, 2004, pp. 388-395.
18. Adams MA, Bogduk N, Burton K. *The Biomechanics of Back Pain*. Edinburgh, Churchill Livingstone, 2002.
19. Wagner H, Anders CH, Puta CH, Petrovitch A, M´orl F, Schilling N, Witte H, Blickhan R. Musculoskeletal support of lumbar spine stability. *Pathophysiology*. 2005;12:257-65.
20. Arjmand N, Shirazi-Adl A. Model and in vivo studies on human trunk load partitioning and stability in isometric forward flexions. *Journal of Biomechanics*. 2006;39:510-21.

21. Benno MN and Herzog W. *Biomechanics of the Musculo-skeletal System*. 2nd Ed, Chichester. Wiley, 1999, pp. 189-198, 71-5.
22. Langton CM and Njeh CF. *The Physical Measurement of Bone*. London, Institute of Physics, 2004.
23. Ruegsegger P, et al. The ability for three-dimensional structural indices to reflect mechanical aspects of trabecular bone. *Bone*. 1991;1:55-60.
24. Stewart TD and Hall RM. Basic biomechanics of human joints: hips, knees and the spine. *Journal of Current Orthopaedics*. 2006;20:23-31.
25. Fagan MJ, *Finite Element Analysis: Theory and Practice*. London, Prentice Hall, 1992, p. xvi.
26. Katz J, Yoon H, Lipson S, Maharidge R, Meunier A, Christel P. The effects of remodeling on the elastic properties of bone. *Calcified Tissue International*. 1984;36:S31-6.
27. Yoon H, Katz J. Ultrasonic wave propagation in human cortical bone. II Measurements of elastic properties and microhardness. *Journal of Biomechanics*. 1976;9:459-64.
28. Ashman RB, Cowin SC, Van Buskirk WC and Rice JC. A continuous wave technique for the measurement of the elastic properties of cortical bone. *Journal of Biomechanics*. 1984;17:349-61.
29. Pithioux M, Lasaygues P and Chabrand P. An alternative ultrasonic method for measuring the elastic properties of cortical bone. *Journal of Biomechanics*. 2002;32:961-968.
30. Minkowsky I and Minkowsky R. The spine, an integral part of the lower extremity. *Clinical Biomechanics of The Lower Extremities*. 1996;1:96.
31. Doblare M, García JM. Application of an anisotropic bone-remodelling model based on a damage-repair theory to the analysis of the proximal femur before and after total hip replacement. *Journal of Biomechanics*. 2001;34:1157-70.